# Thermodynamic evaluation of a combined ORC-TFC cycle for power generation from solar and other low-temperature energy sources

**M.M. El-Awad**
**Independent researcher**

This paper presents a thermodynamic evaluation of a combined power generation cycle for recovering the energy of low-temperature heat sources such as solar energy and industrial waste energy. The cycle connects the simple Organic Rankine Cycle (ORC) with the Trilateral Flash Cycle (TFC) via a cascade condenser. By applying the TFC in the high-temperature circuit and the ORC in the low-temperature circuit, the combined cycle enjoys the merits of the two subsidiary cycles. For evaluating the thermodynamic performance of the cycle, an Excel-based model is described that determines the fluid properties by using special functions developed by VBA. The accuracy of the functions is checked by comparing their estimations with relevant published data for the basic ORC and TFC using a number of relevant fluids. The performance of the combined cycle is first evaluated by comparison with those of the simple TFC and ORC with R152a as the working fluid in all three cycles. It is then evaluated with five fluids of low GWP which are R1234yf in the ORC circuit and R152a, R600, R600a, or R717 in the TFC circuit.

## 1. Literature review

The mounting concerns about the damage to the environment and the climate changes due to the use of fossil-fuels for electricity generation have inspired intensive research for the development of new technologies that utilise alternative energy sources such as solar and geothermal energy and waste heat from industries. One of the promising technologies for the utilisation of such energy sources is the organic Rankine cycle (ORC) [1-3]. Unlike the conventional Rankine cycle that requires steam at very high temperatures before expanding in the turbine, the ORC can be adapted to heat sources at low and moderate temperatures by using an organic fluid as the working fluid instead of steam. Efficiency is the main concern about the cycle and, like the conventional cycle, various modifications to the simple ORC have been considered for improving it such as reheating, regeneration, and recuperation [1]. Although such modifications are effective, they do not address an inherent drawback of the ORC which is the mismatch between the temperature of a finite heating source and that of the working fluid during the heat-addition process in the evaporator since the temperature of the working fluid remains constant while that of the heating source drops [4]. To solve this problem, the trilateral flash cycle has been proposed. In this cycle the saturated liquid fluid is not allowed to vaporise during the heat recovery process but taken directly to expand in a two-phase expander [4-7]. However, the technology of TFC expanders is relatively immature and, therefore, they are less efficient compared to the conventional turbines [1,5].

Most previous researchers developed theoretical models for comparing the performance of the ORC and TFC from thermodynamics and thermoeconomic viewpoints or compared them with other cycles such as the Kalina cycle. For example, Bidgoli and Yanagihara [2] analysed an ORC system to recover the waste heat from the intercoolers of the compression units of a large processing plant. By using Aspen HYSYS, they compared the performance of various working fluids including R123, n-butane, n-pentane, hexane, and n-heptane. Their results showed that a net power of up to 40 MW could be generated with R123. Wolf et al. [3] investigated a solar powered ORC using pure iso-pentane and two iso-pentane/$CO_2$ zeotropic mixtures. Modelling of the system was done by using EES (engineering equation solver) software while determining the thermodynamic properties by using REFPROP. They conducted both exergy and exergo-economic analyses and their study showed that the investigated unit was capable of co-producing approximately 30 kW electricity and 160 kW district heating with a exergetic efficiency exceeding 60%. Therefore, the unit was able to compete with existing renewable power generating systems in terms of specific cost of electricity.

Skiadopoulos et al. [4] assessed the potential of the TFC as a promising higher efficiency alternative to the ORC for solar energy exploitation. The system they studied consisted of a field of evacuated tube collectors

and a TFC engine. To develop their analytical model, the thermodynamic properties of the fluids involved were calculated by using the CoolProp library wrapper for Matlab. Yari et al. [5] considered a low-grade heat source with a temperature of 120°C and conducted parametric studies for several working fluids in ORC and TFC cycles by using the EES software. Their results showed that increasing the inlet temperature of the TFC expander increases the net output power and decreases the product cost, but this was not the case for the ORC system. Lykas et al. [6] compared two innovative designs feeding with the same low-temperature (80-100°C) heat source. The first design was an ORC system in which a small fraction of the supplied waste heat was continuously provided to the expander with the aim of approaching a quasi-isothermal process instead of the adiabatic one. The second design was the TFC. They performed parametric thermodynamic analyses of the two cycles, with R1234ze(E), R1234yf, R1233zd(E), and R134a as working fluids through Aspen Plus software. Their techno-economic study of this cycle conducted by using Aspen Process Economic Analyzer (APEA) with the four working fluids showed that R1233zd(E) was the most proper working fluid for the cycle.

Some researchers studied the utilisation of the ORC for cogeneration. For example, Sun et al. [8] investigated the ORC cycle combined with the Absorption Refrigeration Cycle (ARC) and the Ejector Refrigeration Cycle (ERC) to recover the waste heat from the flue gas for generating both power and cooling for external uses. Their results, with R113 as the working fluid, showed that the net power output, refrigerating capacity, and exergy efficiency of the ORC-ARC combination are all higher than those of the ORC-ERC combination for evaporation temperatures of the basic ORC exceeding 153°C. Toujani et al. [9] combined the ORC with the vapour compression refrigeration (VCR) cycle for cogeneration with a negative cold (-10–0◦C) and a positive cold (0–10◦C) applications. They examined three configurations in terms of the net power, refrigeration capacity and overall efficiency and they used n-hexane as working fluids for the ORC and R600 for the VCC. Their results obtained by using the EES software showed that, for a hot spring of 1000 kW, the cycle could provide simultaneously, a maximum net work of 17 kW and a maximum net cooling capacity of 160 kW and an overall coefficient of the order of 0.3. For the production of positive cold, their results showed that the basic ORC cycle (without recovery) was the most suitable option.

Few researchers reported the results of theoretical studies of cascade ORC systems or hybrid systems involving ORC with steam turbines. For example, Oko et al. [10] presented exergoeconomic analysis of a 100 kW solar driven ORC power plant. They considered a cascade cycle of R134a and R290 as working fluids and developed their model in Microsoft Excel and MATLAB environments. They determined the energy and exergy efficiencies of the proposed plant at the optimal collector operation as 18.92 and 21.61%, respectively. Najjar and Qatramez [11] modelled a hybrid system consisting of a single flash geothermal cycle operating on a steam turbine and ORC using n-butane, isobutane, R11, and R123. The highest energy efficiency of 18.76% and net power output of 24,887MW were obtained with R11. Mokarram and Mosaffa [12] studied a cycle that integrated a steam turbine and a trans-critical ORC using R245fa. They showed that the system could produce 7.2% more power compared to a similar cycle operating in subcritical conditions. With a maximum energy and exergy efficiencies of 14.66% and 55.15%, respectively, the system's LCOE was 0.2018 USD/kWh. Liu et al. [13] studied a two stage subcritical saturated ORC system with a heat source temperature of 100~150 C with four different organic working fluids. The EES software was used to study the ORC power generation system.

The brief literature review given above and the more comprehensive review given in [14] indicate that a cycle that combines the TFC in the high-temperature circuit (HTC) and the ORC in the low-temperature circuit (LTC) has not been considered before. While minimising the mismatch between the working fluid and the heat source for the ORC, the new cycle enables a turbine to be used in the LTC instead of the two-phase expander that, according to [4, 5, and 6], is the main factor for degrading the efficiency of the TFC. Moreover, different organic fluids can be used in the HTC and LTC that suit the high and low temperature ranges better than a single fluid. Needless to say that such a cycle also gives cogeneration systems more flexibility than a single ORC or LTC. In this regard, the present paper contributes to knowledge by presenting a thermodynamic evaluation and multi-objective optimisation of this new cycle using a single

working fluid as well as various environment-friendly fluids. From another perspective, the literature review shows that most researchers used commercial software for their analyses. However, the use of general-purpose software can encourage independent researchers and engineering students to contribute to the development of innovative ORC and TFC systems using suitable fluids [15, 16]. In this respect, the model used in the present study uses Microsoft Excel as the modelling platform with special VBA functions to determine the thermodynamic properties of the working fluids. While the versatile solver that comes with Excel can be used for single-objective optimisation analyses, the free version of the MIDACO solver [17,18] or the Solver-TOPSIS technique described in [19] can be used for multi-objective optimisation analyses.

## 2. The ORC, TFC, and the proposed combined ORC-TFC cycle

Figure 1 shows schematic diagrams of the simple ORC and TFC systems and Figure 2 shows their respective *T-s* diagrams. As Figure 1.a shows, the ORC system has the same components as those of the conventional Rankine cycle which are the evaporator (boiler), the turbine, the condenser, and the pump. Organic fluids are used in the ORC instead of water because they have higher boiling pressures at low temperatures and, therefore, suit the low-temperature applications better. To avoid the problem of blade erosion at the last turbine stages, dry or isentropic fluids are usually selected for which the saturated liquid-vapour curves have negative or infinite slopes, respectively [1,13].

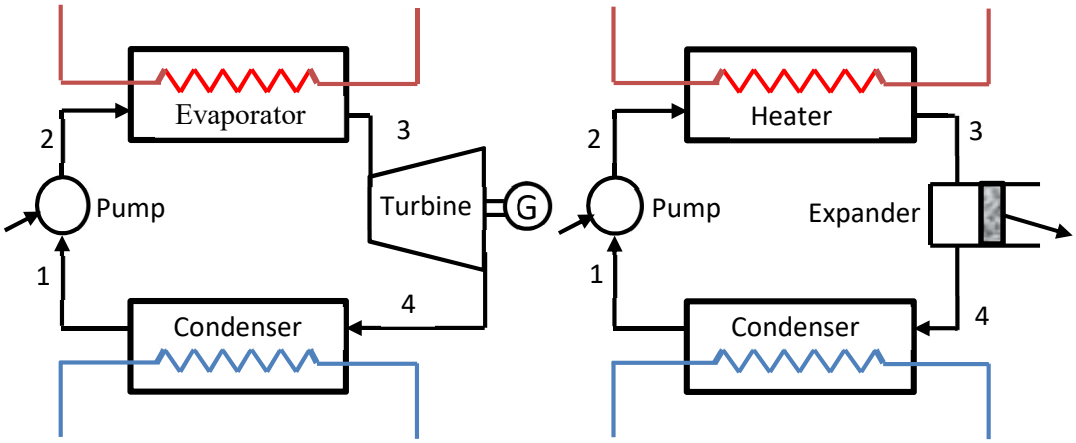


(a) (b)

Figure 1. Schematic diagrams of: (a) the ORC system and (b) the TFC system

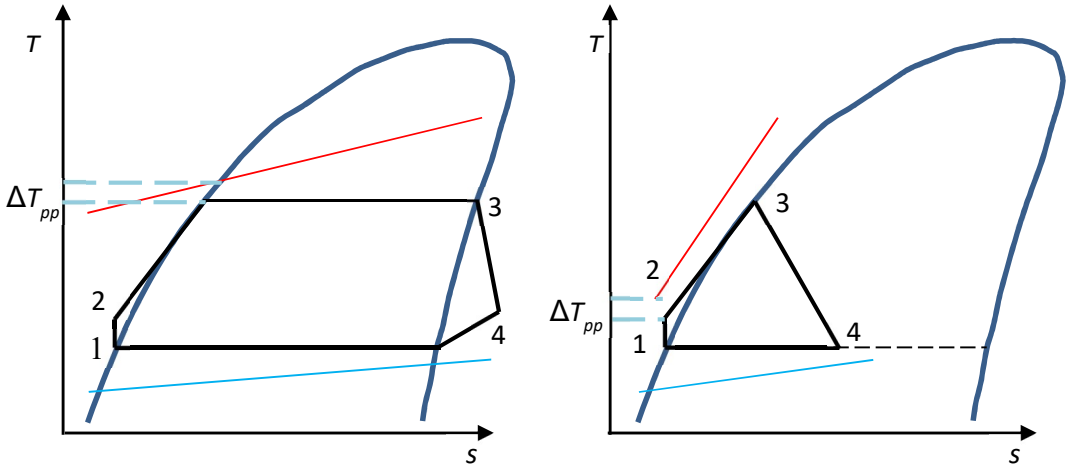


(a) (b)

Figure 2. *T-s* diagrams of: (a) the ORC cycle and (b) the TFC cycle

The TFC system is different from the ORC system in that it heats the working fluid without going into the vaporisation process so that the hot pressurised fluid expands in the two-phase region. As Figure 2.b shows, this cycle leads to a uniform temperature glide between the heat source and the working fluid; which reduces the losses during the heat-transfer process and improves the performance of the TFC systems. Typically, TFC systems can provide 50% more work than ORC systems for the same energy input, but they need sophisticated expanders that can adequately handle the liquid-phase presence during the expansion process [1]. Apart from increasing the investment cost, two-phase expanders are generally less efficient than conventional vapour turbines.

Figure 3.a shows a schematic diagram of the combined-cycle system in which the heat source is first used to heat the working fluid of the TFC circuit and then heat the working fluid of the ORC circuit. After expanding in the two-phase expander to produce power, the working fluid of the TFC circuit is condensed by the cooler working fluid of the ORC circuit in a cascade condenser (cc) before being pumped into the TFC heater. The ORC system shown on Figure 3.a is a recuperative system in which the superheated fluid exiting the turbine is used to heat the cold fluid exiting the pump in an internal heat-exchanger (IHEX). In the condenser, the working fluid is cooled by the cold-sink fluid to the saturated-liquid state and then pumped into the cold side of the IHEX. After the IHEX, the fluid is heated by the heat source to the state of saturated liquid before entering the cascade condenser where it is heated further by the condensing fluid of the TFC circuit until it becomes saturated vapour.

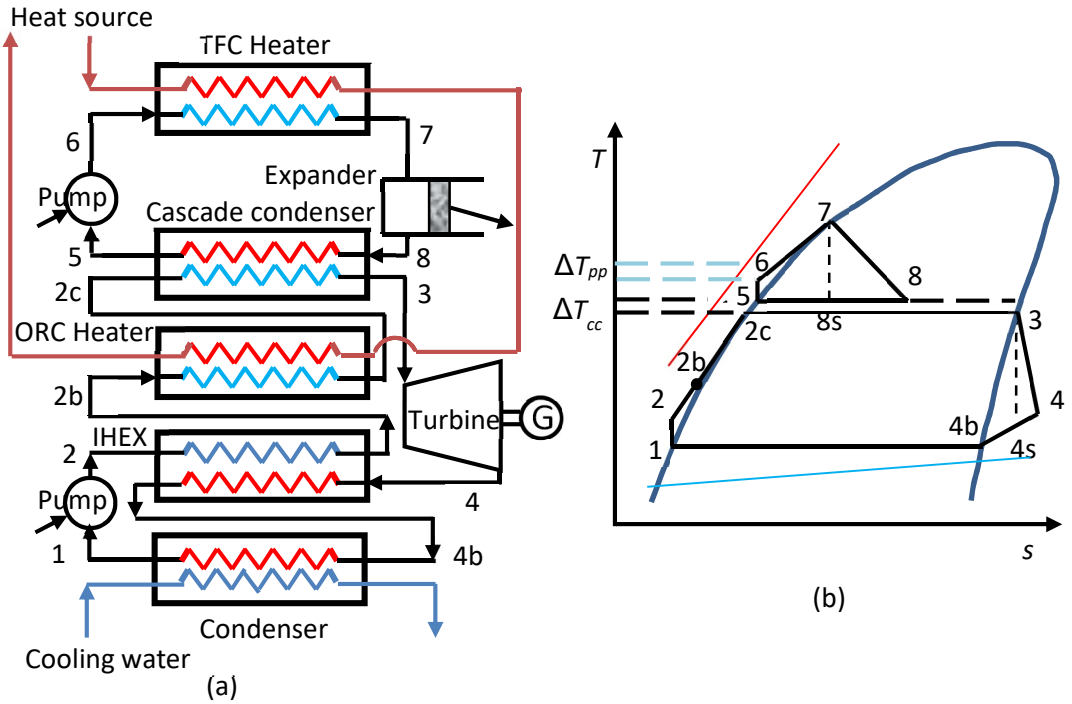


Figure 3. Schematic and *T-s* diagrams for the combined ORC-TFC cycle

Figure 3.b shows the *T-s* diagram of the combined cycle. Unlike the TFC cycle in which the pinch point occurs where the heating fluid exits the system, that of the combined cycle occurs in the middle of the heating process which forces the heating source to exit the system at a higher temperature than that of the TFC. Although this limits the amount of heat recovered and the work produced by the ORC circuit, the combined cycle can still produce more work than the simple ORC alone because of the additional work produced by the TFC circuit. Compared to a simple TFC, the combined cycle may not be able to produce the same power but it can have a higher thermal efficiency by replacing the two-phase expander with the single-phase turbine and by allowing two different working fluids to be used in the TFC and ORC circuits that lead to a better overall performance than a single fluid.

## 3. The analytical model for the combined cycle

The analytical model for the present thermodynamic analyses assumes steady-state operation and neglect pressure losses and heat-transfer losses in the various components. However, the losses due to irreversibility in the pumps, the turbine, and the two-phase expander are taken into consideration via the relevant isentropic efficiencies [20].

### 3.1. The analytical model for the TFC circuit

Given the pinch-point temperature difference, $\Delta T_{pp}$, the temperature of the heat source exiting the heater of the TFC, $T_{hso,TFC}$, is determined from:

$$T_{hso,TFC} = T_6 + \Delta T_{pp} \tag{1}$$

Given the inlet temperature of the heat source, $T_{hs,in}$, and its mass flow rate, $\dot{m}_{hs}$ , the rate of heat transfer from the heat source (a stream of hot-water) to the working fluid of the TFC, $\dot{Q}_{hs,TFC}$ , and the mass flow rate of the working fluid, $\dot{m}_{TFC}$ , are calculated from:

$$\dot{Q}_{hs,TFC} = \dot{m}_{hs} c_p \left(T_{hs,in} - T_{hso,TFC}\right) \tag{2}$$

$$\dot{m}_{TFC} = \dot{Q}_{hs,TFC} / \left(h_7 - h_6\right) \tag{3}$$

The specific work, in kJ per kg, of the working fluid in the TFC during the two-phase expansion process is evaluated from the enthalpy change as follows:

$$w_{exp} = \left(h_7 - h_{8s}\right) \times \eta_{exp} \tag{4}$$

Where $\eta_{exp}$ is the isentropic efficiency of the expander and $h_{8s}$ is the enthalpy of the fluid after an isentropic expansion (refer to Figure 3.b). The TFC pump specific work is given by:

$$w_{p,TFC} = v_5 \left(p_{eva,TFC} - p_{cc,TFC}\right) / \eta_{p,TFC} \tag{5}$$

Where $p_{eva,TFC}$ and $p_{cc,TFC}$ are the pressures of the TFC fluid in the evaporator and cascade-condenser, respectively. Equation (6) is then used to determine the enthalpy of the fluid at state 6 after the pump:

$$h_6 = h_5 + w_{p,TFC} \tag{6}$$

The thermal efficiency of the TFC circuit alone is given by:

$$\eta_{TFC} = \dot{m}_{TFC} \left(w_{exp} - w_{p,TFC}\right) / \dot{Q}_{hs,TFC} \tag{7}$$

### 3.2. The analytical model for the ORC circuit

Referring to Figure 3b, the mass flow rate of the working fluid in the ORC circuit is given by:

$$\dot{m}_{ORC} = \dot{m}_{TFC} \left(h_8 - h_5\right) / \left(h_3 - h_{2c}\right) \tag{8}$$

The pump specific work is given by:

$$w_{p,ORC} = v_1 \left(p_{cc,ORC} - p_{con,ORC}\right) / \eta_{p,ORC} \tag{9}$$

Where $\eta_{p,ORC}$ is the isentropic efficiency of the ORC pump. Energy balance over the IHEX gives:

$$h_{2b} = h_2 + (h_4 - h_{4b}) \tag{10}$$

Where $h_{4b}$ is the enthalpy of the saturated vapour at the condenser pressure. The enthalpy $h_4$ is determined by taking into consideration the irreversibility of the turbine as follows:

$$h_4 = h_3 + (h_3 - h_{4s}) \times \eta_t \tag{11}$$

Where $h_{4s}$ is the enthalpy after an isentropic expansion and $\eta_t$ is the isentropic efficiency of the turbine. The turbine's specific work is then calculated from:

$$w_t = h_3 - h_4 \tag{12}$$

The thermal efficiency of the ORC circuit alone is given by:

$$\eta_{ORC} = \dot{m}_{ORC}(w_t - w_{p,ORC}) / \dot{Q}_{hs,TFC} \tag{13}$$

Where $\dot{Q}_{hs,ORC}$ is the heat recovered in the ORC circuit, which is given by:

$$\dot{Q}_{hs,ORC} = \dot{m}_{ORC}(h_{2c} - h_{2b}) \tag{14}$$

### 3.3. The analytical model for the combined cycle

The total heat recovered from the heat source and total net power produced by the combined cycle, respectively, are given by:

$$\dot{Q}_{hs,tot} = \dot{Q}_{hs,TFC} + \dot{Q}_{hs,ORC} \tag{15}$$

$$\dot{W}_{tot} = \dot{m}_{ORC}(w_t - w_{p,ORC}) + \dot{m}_{TFC}(w_{exp} - w_{p,TFC}) \tag{16}$$

The overall thermal efficiency and the second-law (exergetic) efficiency of the cycle are given by:

$$\eta_{tot} = \dot{W}_{tot} / \dot{Q}_{hs,tot} \tag{17}$$

$$\varepsilon_{tot} = \dot{W}_{tot} / \dot{E}_{hs,in} \tag{18}$$

Where $\dot{E}_{hs,in}$ in Equation (18) is the rate of exergy flow of the heat source entering the system following the definition adopted by Yari et al. [5]:

$$\dot{E}_{hs,in} = \dot{m}_{hs}[(h_{hs,in} - h_0) - T_0(s_{hs,in} - s_0)] \tag{19}$$

The temperature of the heat source exiting the system is given by:

$$T_{hs,out} = T_{hs,in} - \dot{Q}_{hs,tot} / \dot{m}_{hs} c_p \tag{20}$$

Where $c_p$ is the specific heat of the heating medium.

## 4. Development and validation of the Excel model

The Excel-based model developed for the present analyses determines the thermal fluid properties by using special user-defined functions developed with VBA [21]. The functions for saturated liquids and saturated vapours interpolate the data given by ASHRAE [22], but he functions that determine the enthalpy and entropy of superheated refrigerants use ideal-gas equations in which the specific heat is determined at an adjusted pressure by multiplying the actual pressure by a "compressibility factor" for which an average value of 0.5 is adopted [23]. Although this approximation enables the functions to be used for supercritical conditions, the accuracy of the functions has to be verified.

### 4.1.1. The ORC model and its validation

Yari et al. [5] analysed the simple ORC with a heat source at 120°C with the data shown on Table 1. Their results for seven working fluids, which are: R134a, R1234yf and R152a, propane (R290), n-butane (R600), iso-butane (R600a), and ammonia (R717), were used to verify the VBA property functions for this cycle and Figure 4 shows the Excel-aided model developed for the system.

Table 1. Values of the parameters used for validating the simple ORC model [5]

| Parameter | Value |
|---|---|
| $T_{hs}$ (°C) | 120 |
| $\dot{m}_{hs}$ (kg/s) | 100 |
| $T_{cond}$ (°C) | 40 |
| $\Delta T_{pp}$ (K) | 10 |
| $\eta_p$ (%) | 85 |
| $\eta_t$ (%) | 85 |

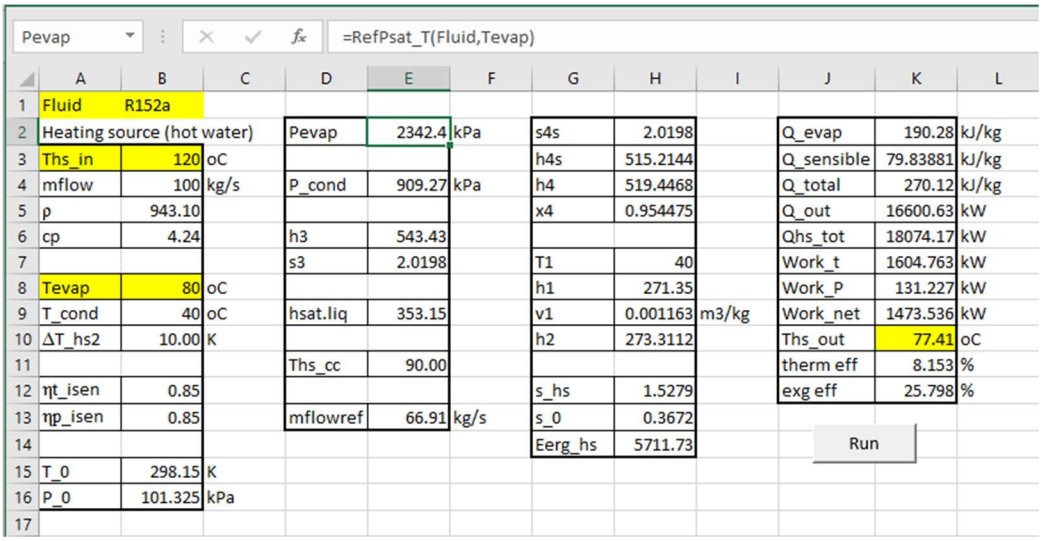


Figure 4. The Excel-aided model for the simple ORC with the data given by [5]

The sheet consists of four blocks of cells. The first block on the left side of the sheet stores the specified data, while the second and third blocks in the middle perform the calculations for the ORC cycle. The fourth block on the right side of the sheet determines the overall cycle parameters that include the total amount of recovered heat (Qhs_tot), the net power produced by the system (Work_net), the exit temperature of the heating source (Ths_out), and the overall energetic (therm_eff) and exergetic (exg_eff) efficiencies. The sheet uses R152a as the working fluid, but the name of the fluid is stored as a variable so that it can be used for other fluids. By using the model, the system's power output, thermal efficiency, and exergetic efficiency were calculated at various values of the turbine's inlet temperature, $T_3$. The results obtained by the present model for the seven fluids are compared on Figures 5 and 6 with those obtained by Yari et al [5] who developed their model by using the EES software. The two figures show close agreement between the results of the present model and their model.

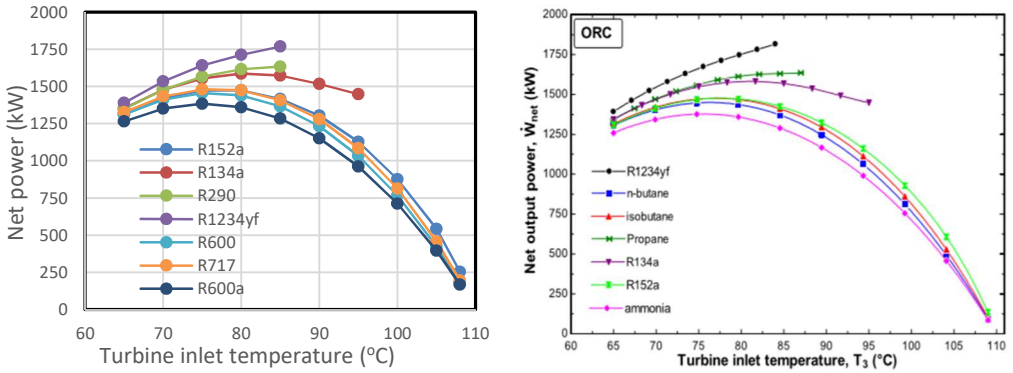


(a) (b)

Figure 5. Comparison of (a) the model's estimations for the net power of the ORC at various values of $T_3$ with (b) the reference [5]

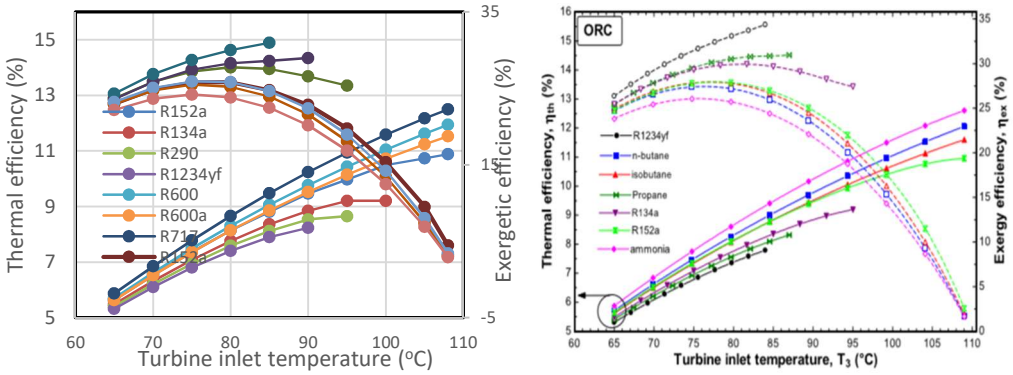


(a) (b)

Figure 6. Comparison of (a) the model's estimations for thermal efficiency and exergetic efficiency of the ORC at various values of $T_3$ with (b) the reference [5]

### 4.1.2. The TFC model and its validation

Figure 7 shows the model developed for the TFC using the data provided by Lai et al. [6] who analysed the cycle with a heat source at 80°C. In their analyses, the mass flow rate of the heat source was 4.16 kg/s, the heat sink temperature was maintained at 30°C, the fluid's inlet temperature to the condenser was 37°C, and the isentropic efficiency of the pump was 0.7. Lai et al. [6] fixed the operating temperature at the inlet of the pump ($T_2$) at 35°C. The model shown on Figure 7 uses the same data, but $T_2$ is evaluated by the model and not fixed.

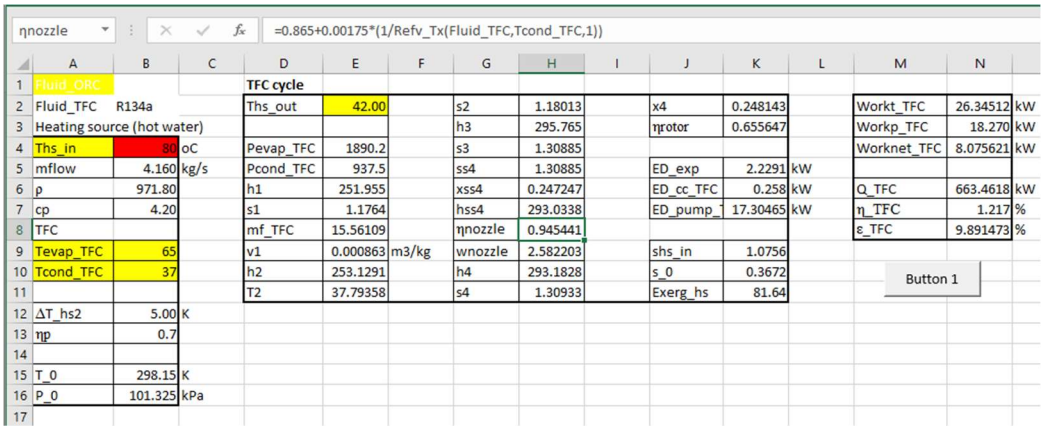


Figure 7. The Excel-aided model for the TFC using R134a with the data of [6]

For their analyses, Lai et al. [6] selected four working fluids that are commonly used in low-grade power generation systems, which are R134a, R236fa, R245fa, and R1233zd. They evaluated the fluid properties by using the REFPROP software. Since R236fa is not supported by the present VBA functions, comparison will be made with the other three fluids, which are R134a, R245fa, and R1233zd. Figure 8. that shows the results obtained by the present model also shows a close agreement with the results of the reference model shown on Figure 9. The results of both models show that R236fa and R1233zd have comparable power and thermal efficiency, but R134a has considerably lower values.

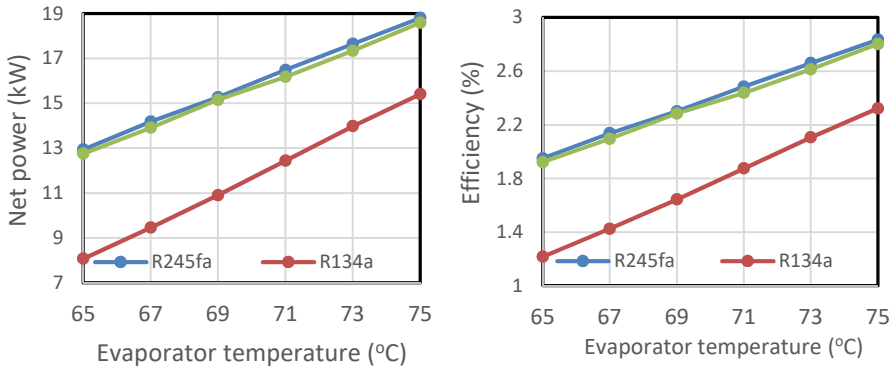


(a) (b)

Figure 8. Variations of the net power and thermal efficiency of the TFC with the evaporation temperature as obtained by the present model

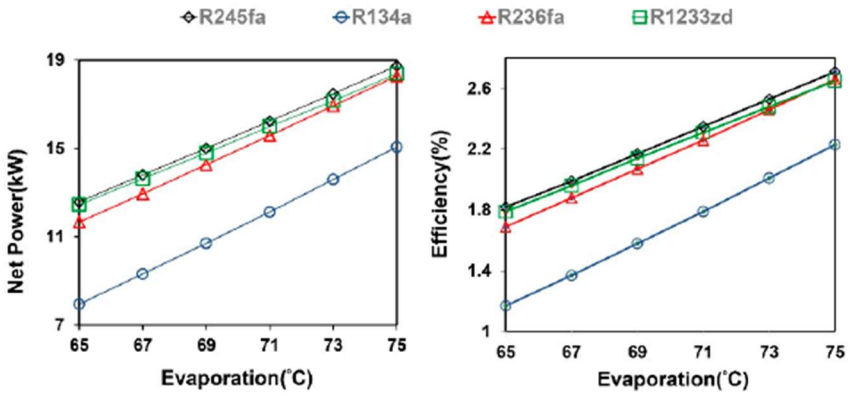


(a) (b)

Figure 9. Variations of the net power and thermal efficiency of the TFC with the evaporation temperature as given by Lai et al. [6]

### 4.1.3. The combined-cycle model

Figure 10 shows the model developed for the combined cycle. The figure shows four blocks of cells the first of which on the left side of the sheet stores the specified data, while the second and third blocks in the middle perform the calculations for the TFC and ORC circuits, respectively. The fourth block on the right side of the sheet determines the overall cycle parameters. The figure shows that R152a is used in both the TFC and ORC circuits, but the names of the working fluids in the two circuits are treated as variables so that the model can be used for different fluid pairs. The temperature of the TFC fluid in the cascade condenser, Tcc_TFC, is specified as 83°C so that, with a cascade-condenser temperature difference of 3°C, that of the ORC fluid, Tcc_ORC, is 80°C.

By fixing value of the temperature of the TFC fluid entering the expander at 110°C, the power, thermal efficiency, and exergetic efficiency of the combined cycle were calculated at various values of the cascade-condenser temperature in the cycle with R152a as the single working fluid. The results are plotted on Figure 11 which shows that the thermal efficiency of the combined cycle increases steadily with the temperature

of the ORC fluid in the cascade condenser, while its power drops. The figure also shows that the exergetic efficiency has a maximum value at the cascade temperature of 75°C. Clearly, the combined cycle has a certain cascade temperature that gives the best trade-off between its produced power, thermal efficiency, and exergetic efficiency.

Pevap_TFC | =RefPsat_T(Fluid_TFC,Tevap_TFC)

| | A | B | C | D | E | F | G | H | I | J | K | L | M | N | O |
|---|---|---|---|---|---|---|---|---|---|---|---|---|---|---|---|
| 1 | **Working fluids** | | | **TFC cycle** | | | | | | | | | **TFC** | | |
| 2 | Fluid_TFC | R152a | | T_hsi | 93.00 | | s6 | 1.508015 | | h8 | 434.86189 | | Workt_TFC | 656.4599 | kW |
| 3 | Fluid_ORC | R152a | | | | | h7 | 439.22 | | s8 | 1.7098828 | | Workp_TFC | 433.9989 | kW |
| 4 | **Heating source (hot water)** | | | Pevap_TFC | 4243.2 | | s7 | 1.7058 | | | | | Worknet_TFC | 222.4611 | kW |
| 5 | T_hs | 120 | oC | Pcc_TFC | 2503.08 | | | | | | | | Q_TFC | 11458.8 | kW |
| 6 | mflow | 100 | kg/s | h5 | 360.266 | | ss8 | 1.7058 | | | | | η_TFC | 1.941 | % |
| 7 | ρ | 943.10 | kg/m3 | s5 | 1.50023 | | xss8 | 0.40023 | | | | | | | |
| 8 | cp | 4.24 | kJ/kg.K | mf_TFC | 150.62947 | | hss8 | 433.4092 | | s_hs | 1.5279 | | **ORC** | | |
| 9 | **TFC** | | | v5 | 0.0014074 | m3/kg | | | | s_0 | 0.3672 | | Q_sensible | 91.67203 | kJ/kg |
| 10 | Tevap_TFC | 110 | oC | h6 | 363.1472 | | | | | Exerg_hs | 3472.92 | | Q_ORC | 5413.38 | kW |
| 11 | Tcc_TFC | 83 | oC | T6 | 84.214554 | | | | | | | | Workt_ORC | 1416.248 | kW |
| 12 | ΔTcc | 3 | K | **ORC cycle** | | | | | | | | | Workp_ORC | 115.811 | kW |
| 13 | ΔT_hs2 | 10 | K | Tcc_ORC | 80 | oC | s4s | 2.0198 | | h2 | 273.31119 | | Worknet_ORC | 1300.436 | kW |
| 14 | **ORC** | | | Pcc_ORC | 2342.4 | kPa | h4s | 515.2144 | | T2 | 41.037827 | | η_ORC | 7.811 | % |
| 15 | Tcond_ORC | 40 | oC | Pcond_ORC | 909.27 | kPa | h4 | 519.4468 | | s2 | 1.2472232 | | | | |
| 16 | ΔT_sc | 0.00 | K | | | | T4 | 40 | | | | | **Overall parameters** | | |
| 17 | ηt_isen | 0.85 | | h3 | 543.43 | | s4 | 2.033315 | | h2b | 261.47797 | | Q_total | 16872.18 | kW |
| 18 | ηp_isen | 0.85 | | s3 | 2.0198 | | | | | T2b | 34.724121 | kJ/kg | T_hsout | 80.24 | oC |
| 19 | ηx_isen | 0.75 | | h2c | 353.15 | | T1 | 40 | oC | s2b | 1.2098085 | kg/s | Q_out | 15349.28 | kW |
| 20 | T_0 | 298.15 | K | s2c | 1.481 | | h1 | 271.35 | kJ/kg | | | | | | |
| 21 | P_0 | 101.325 | kPa | | | | v1 | 0.001163 | m3/kg | Qevap_ORC | 190.28 | kW | W_total | 1522.897 | kW |
| 22 | | | | h4b | 531.28 | | s1 | 1.2411 | | mf_ORC | 59.05 | kW | η_overall | 9.026 | % |
| 23 | | | | s4b | 2.0711 | | | | | | | | ε_overall | 43.85063 | % |
| 24 | | | | | | | | | | | | | | | |

Figure 10. Excel-aided model for the combined cycle using R152a with the data shown on Table 1

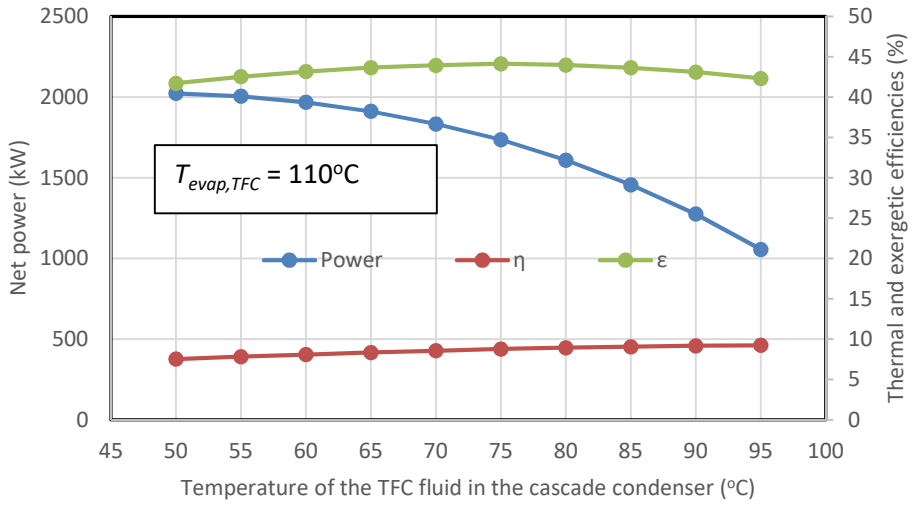


Figure 11. Variation of the combined-cycle's power and thermal and exergetic efficiencies with the temperature of the TFC fluid in the cascade condenser

## 5. Comparison with the simple ORC and TFC

The performance of the combined cycle will be compared to that of the ORC and TFC cycles using the same working fluid in all three cycles, which is R152a. The comparison will be for a heat-source at 120°C and using the data shown on Table 1. In order to make comparison with the TFC at a heat-source of 120°C, the TFC model shown on Figure 7 has to be modified. Figure 12 shows the modified TFC model with R152a as the working fluid and using the input data of Table 1. The temperature of the TFC fluid entering the TFC expander is taken as 110°C for both the TFC and the combined cycle and the isentropic efficiency of the TFC expander is specified as 75% for both cycles. Also note that the condenser temperature for the TFC is now 40°C and the pinch-point temperature difference is 10°C. Since Figure 5 shows that the ORC has a certain temperature in its evaporator that maximises its output power, which is 80°C, the comparison with the ORC will be based on the cycle's performance at this temperature as shown on Figure 4.

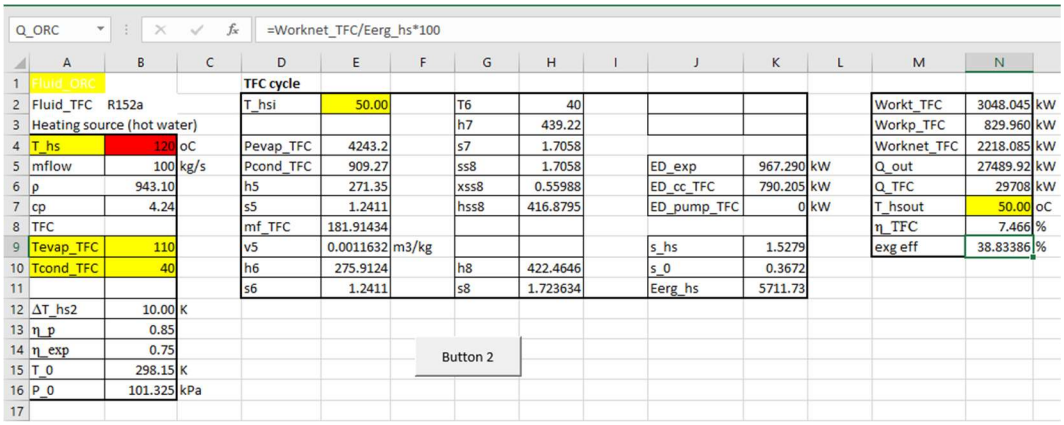


| | | | | | | | | | | | | | | | |
|---|---|---|---|---|---|---|---|---|---|---|---|---|---|---|---|
| 1 | Fluid_ORC | | | TFC cycle | | | | | | | | | | | |
| 2 | Fluid_TFC | R152a | | T_hsi | 50.00 | | T6 | 40 | | | | | Workt_TFC | 3048.045 | kW |
| 3 | Heating source (hot water) | | | | | | h7 | 439.22 | | | | | Workp_TFC | 829.960 | kW |
| 4 | T_hs | 120 | oC | Pevap_TFC | 4243.2 | | s7 | 1.7058 | | | | | Worknet_TFC | 2218.085 | kW |
| 5 | mflow | 100 | kg/s | Pcond_TFC | 909.27 | | ss8 | 1.7058 | | ED_exp | 967.290 | kW | Q_out | 27489.92 | kW |
| 6 | ρ | 943.10 | | h5 | 271.35 | | xss8 | 0.55988 | | ED_cc_TFC | 790.205 | kW | Q_TFC | 29708 | kW |
| 7 | cp | 4.24 | | s5 | 1.2411 | | hss8 | 416.8795 | | ED_pump_TFC | 0 | kW | T_hsout | 50.00 | oC |
| 8 | TFC | | | mf_TFC | 181.91434 | | | | | | | | η_TFC | 7.466 | % |
| 9 | Tevap_TFC | 110 | | v5 | 0.0011632 | m3/kg | | | | s_hs | 1.5279 | | exg eff | 38.83386 | % |
| 10 | Tcond_TFC | 40 | | h6 | 275.9124 | | h8 | 422.4646 | | s_0 | 0.3672 | | | | |
| 11 | | | | s6 | 1.2411 | | s8 | 1.723634 | | Eerg_hs | 5711.73 | | | | |
| 12 | ΔT_hs2 | 10.00 | K | | | | | | | | | | | | |
| 13 | η_p | 0.85 | | | | | | | | | | | | | |
| 14 | η_exp | 0.75 | | | | | | | | | | | | | |
| 15 | T_0 | 298.15 | K | | | | | | | | | | | | |
| 16 | P_0 | 101.325 | kPa | | | | | | | | | | | | |
| 17 | | | | | | | | | | | | | | | |

Figure 12. The modified model for the TFC cycle using R152a with the data of Table 1

Table 2 compares the values obtained by the three cycles for a number of performance parameters. For the ORC and TFC cycles, the relevant values are obtained from Figure 4 and Figure 12, respectively. For the combined cycle, three sets of values are shown which correspond to three values of the temperature of the ORC fluid in the cascade condenser, Tcc_ORC, which are 70ºC (CC-70), 80ºC (CC-80), and 90ºC (CC-90). The table figures show that the lowest exit temperature for the heat source is that of the TFC, which is 50ºC, and the highest exit temperature is that of the combined cycle CC-90, which is 90.72ºC.

Table 2. Performance parameters of the ORC, TFC, and the combined cycle

| | TFC | ORC | CC-70 | CC-80 | CC-90 |
|---|---|---|---|---|---|
| Ths,out (ºC) | 50 | 77.41 | 71.75 | 80.24 | 90.72 |
| Qin (kW) | 29708 | 18074.17 | 20479.42 | 16872.18 | 12427.7 |
| Qout (kW) | 27489.92 | 16600.63 | 18700.75 | 15349.28 | 11278.86 |
| Power (kW) | 2218.085 | 1473.536 | 1778.665 | 1522.897 | 1148.837 |
| Thermal efficiency (%) | 7.466 | 8.153 | 8.685 | 9.026 | 9.244 |
| Exergetic efficiency (%) | 38.834 | 25.798 | 31.141 | 43.851 | 20.114 |

Figures 13 and 14 compare amount of heat recovered, power produced, thermal efficiency, and exergetic efficiency of the three cycles. Figures 13 shows that the simple TFC recovers the most energy and produces the most power compared to the other two cycles. The figure also shows that both the heat recovered and power produced by the combined cycle decrease as the cascade temperature is increased. The recovered energy and power produced by the combined cycle are lower than those of the TFC for all three cascade temperatures, but higher than that of the ORC for cascade temperatures below 80ºC.

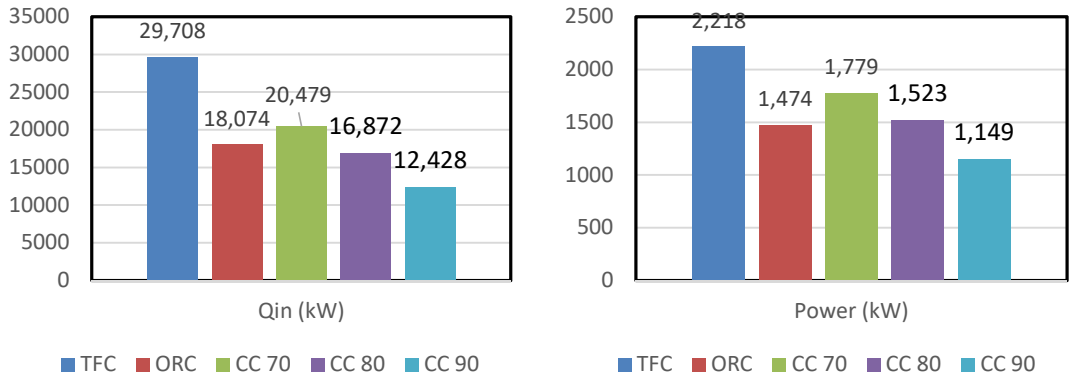


(a) (b)

Figure 13. Comparison of (a) the recovered heating source energy and (b) the power produced by the combined cycle with those of the simple TFC and ORC

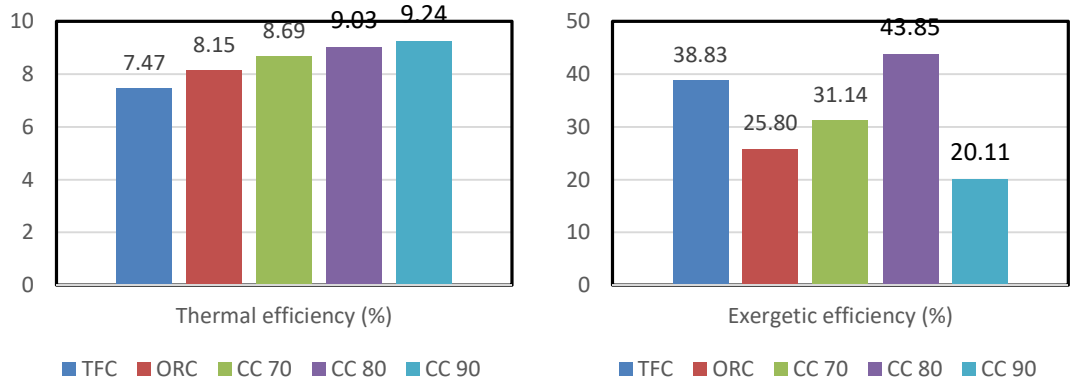


(a) (b)

Figure 14. Comaprison of (a) the and thermal efficiency and (b) the exergetic efficiency of the combined cycle with those of the simple TFC and ORC

An unconditional advantage of the combined cycle is revealed by Figure 14 which is that its thermal efficiency is higher than those of the TFC and ORC cycles at all three cascade temperatures and increases with the cascade temperature. Figure 14.b shows that the exergetic efficiency of the combined cycle at the cascade temperature of 80°C exceeds those for both the simple TFC and ORC cycles. These results support what has been mentioned earlier which is that there is an optimum cascade temperature for the cycle that gives the best trade-off between its power, thermal efficiency and the exergetic efficiency.

## 6. Analysis of the combined cycle with five low-GWP fluids

The evaluation of the combined cycle presented in the previous section did not take into consideration an important advantage of the combined cycle which is the ability to use different working fluids in the TFC and ORC circuits. This section analyses the performance of the combined cycle for the medium-temperature source of 120°C with five fluids that have zero ozone-layer depletion potential (ODP) and low global-warming potential (GWP), which are R152a, R1234yf, R600, R600a, and R717. Table 3 shows their physical characteristics, GWP, and safety groups according to ASHRAE [22].

Table 3. Boiling point, ODP, GWP, and safety group of the five fluids [22]

| Fluid | Normal boiling point (°C) | Critical temperature (°C) | Critical pressure (kPa) | GWP | Safety group |
|---|---|---|---|---|---|
| R1234yf | –29.4 | 94.7 | 3382.2 | <1 | A2L |
| R152a | –24 | 113.26 | 4516.8 | 138 | A2 |
| R600 | 0 | 151.98 | 3796.0 | 4 | A3 |
| R600a | –12 | 134.66 | 3629.0 | ¬20 | A3 |
| R717 | −33.33 | 132.25 | 11,333.0 | 0 | B2L |

Figures 5 and 6 show that R1234yf can achieve the highest power and exergetic efficiency in the lower-temperature range, but it has the lowest thermal efficency. By using R1234yf in the ORC circuit and R152a in the TFC circuit of the combined cycle, the model was used to calculate the power and thermal efficiency of the cycle at various temperatures in the cascade condenser. Figure 15 compares the values obtained by this pair with those of the simple ORC shown on Figures 5 and 6 and those of the combined cycle with R152a in both circuits shown in Figure 11. Figure 15.a shows that both the power and thermal efficiency of the combined cycle with both fluid pairs are higher than those of the simple ORC at values of the cascade temperature below 80°C, i.e., when the contribution of the TFC circuit is dominant. The figure also shows that the power of the combined cycle with the R152a/R1234yf pair remains higher than that of the R152a/R152a pair over the whole range of cascade temperatures. However, Figure 15.b shows that the thermal efficiency of the combined cycle with the R152a/R1234yf pair remains lower than that of the

R152a/R152a pair over the whole range of cascade temperatures. The model was also used to calculate the power and thermal efficiency of the combined cycle with the other three fluid pairs. The percentage deviations of the calculated values of the power and thermal efficiency from those of the R152a/R1234yf pair are shown on Figure 16.

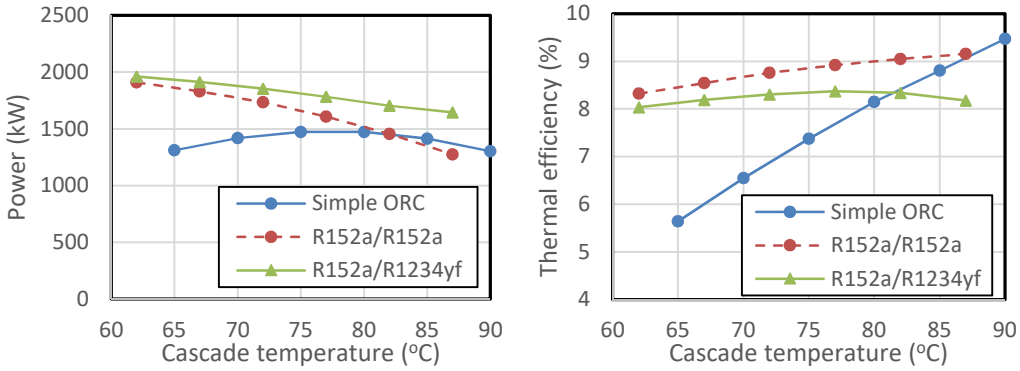


(a) (b)

Figure 15. Comparison of (a) the power and (b) thermal efficiency of the combined cycle with R152a/R1234yf with those with R152a/R152a and the simple ORC

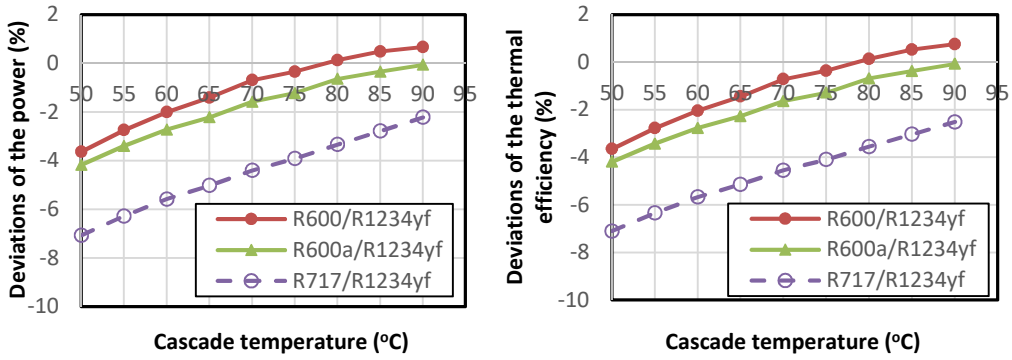


(a) (b)

Figure 16. Percentage deviations of (a) the power and (b) thermal efficiency of the combined cycle with R600, R600a, and R717 in the TFC circuit from those with R152a

Figure 16.a shows that all three pairs produce less power than R152a/R1234yf for cascade temperatures below 80°C, but the lowest values are those of the pair involving R717. For all three fluid pairs, the deficits from the R152a/R1234yf pair diminish steadily as the cascade temperature is increased, but only R600/R1234yf manges to produce more power than R152a/R1234yf at cascade temperatures above 80°C. Figure 16.b shows that the thermal efficiency for each fluid pair deviates from the corresponding values of the R152a/R1234yf pair by the same pecentage as the pair's power.

## 7. Closure

This paper presents a combined cycle for power generation from low-temperature heat sources that utilises the TFC in the high-temperature circuit and the ORC in the low-temperature circuits. By connecting the two circuits via a casket condenser, the combined cycle allows different fluids to be used in the lower and the higher temperature ranges. The performance of the combined cycle is compared to those of the simple TFC and ORC by using an Excel-based model that utilises VBA functions to determine the refrigerants properties. The functions are first validated by comparing their estimations for the simple ORC and TFC with the data obtained from published sources. Then, the combined cycle is compared to the simple ORC and TFC by using R152a in both the HTC and LTC circuits. The results obtained for a heat source available at 120°C show that combined cycle gives more power and yields higher thermal and exergetic efficiencies than the simple ORC for cascade temperatures below 80°C. Compared to the simple TFC, the combined

cycle produces less power, but achieves higher thermal efficiencies for any cascade temperature. The exergetic efficiency of the cycle is also higher than that of the simple TFC at a cascade temperature of 80°C.

Whether the same fluid or different fluids are used in the two circuits of the combined cycle, the various analyses of the cycle show that its thermal efficiency steadily increases by increasing the cascade temperature, but the power decreases while the exergetic efficiency has an optimum cascade temperature. Therefore, selecting the appropriate cascade temperature for the combined cycle requires a trade-off between the power of the cycle on one side and its thermal and exergetic efficiencies on the other side. Determining the most suitable fluid pair for the cycle and the appropriate cascade temperature requires multi-objecve optimisation analyses of the cycle that also take other factors into consideration including the economic, safety, and environmental factors. In this respect, the Excel-based model described in the paper allows the multi-objective optimisation analyses to be conducted by using either the free version of the MIDACO solver [17,18] or the Solver-TOPSIS technique described in [19].

**References**


[1] J.J. Fierro, C. Hern´andez-G´omez, C.A. Marenco-Porto, C. Nieto-Londo˜no, A. Escudero-Atehortua, M. Giraldo, H. Jouhara, L.C. Wrobel, Exergo-economic comparison of waste heat recovery cycles for a cement industry case study, Energy Conversion and Management: X 13 (2022) 100180

[2] A.A. Bidgoli and J.I. Yanagihar, Integration of the Compression Units of the Processing Plant with an Organic Rankin Cycle for Power Generation and Cooling Process, Proceedings of ECOS 2023 - the 36th International Conference on Efficiency, Cost, Optimization, Simulation and Environmental Impact of Energy Systems 25-30 June, 2023, Las Palmas De Gran Canaria, Spain

[3] C. Wolf, E. Rothuizen, T. Ommen, Exergoeconomic Analysis of a Solar Powered ORC using Zeotropic Mixtures for Combined Heat & Power Generation, Proceedings of ECOS 2023 - the 36th International Conference on Efficiency, Cost, Optimization, Simulation and Environmental Impact of Energy Systems 25-30 June, 2023, Las Palmas De Gran Canaria, Spain

[4] A. Skiadopoulos, C. Antonopoulou, K. Atsonios, P. Grammelis, A. Gkountas, P. Bakalis, G. Kosmadakis, and D. Manolakos, Trilateral Flash Cycle for efficient low temperature solar heat harvesting- A case study, Proceedings of ECOS 2023 - the 36th International Conference on Efficiency, Cost, Optimization, Simulation and Environmental Impact of Energy Systems 25-30 June, 2023, Las Palmas De Gran Canaria, Spain

[5] M. Yari, A.S. Mehr, V. Zare, S.M.S. Mahmoudi, M.A. Rosen, Exergoeconomic comparison of TLC (trilateral Rankine cycle), ORC (organic Rankine cycle) and Kalina cycle using a low grade heat source, Energy 83 (2015) 712-722

[6] K-Y. Lai, Y-T. Lee, M-R. Chen and Y-H. Liu, Comparison of the Trilateral Flash Cycle and Rankine Cycle with Organic Fluid Using the Pinch Point Temperature, Entropy (2019), 21, 1197

[7] P. Lykas, C. Antonopoulou, A. Gkountas, K. Atsonios, G. Itskos, N. Nikolopoulos, P. Grammelis, D. Manolakos and P. Bakalis, Thermodynamic and economic performance of novel organic cycle designs powered by low temperature waste heat, Proceedings of ECOS 2023 - the 36th International Conference on Efficiency, Cost, Optimization, Simulation and Environmental Impact of Energy Systems 25-30 June, 2023, Las Palmas De Gran Canaria, Spain

[8] W. Sun, X. Yue, and Y. Wang. Exergy Efficiency Analysis of ORC (Organic Rankine Cycle) and ORC-Based Combined Cycles Driven by Low-Temperature Waste Heat. Energy Conversion and Management, 135, (2017), 63-73. https://doi.org/10.1016/j.enconman.2016.12.042

[0] N. Toujani, N. Bouaziz, M. Chrigui, L. Kairouani, Performance analysis of a new combined organic Rankine cycle and vapor compression cycle for power and refrigeration cogeneration, Transactions of the Institute of Fluid-flow Machinery, No. 140, 2018, 39–81

[10] C.O.C. Oko, M.M. Deebom, and, E.O. Diemuodeke, Exergoeconomic analysis of cascaded organic power plant for the Port Harcourt climatic zone, Nigeria, Cogent Engineering (2016), 3: 1227127, http://dx.doi.org/10.1080/23311916.2016.1227127

[11] Y.S.H. Najjar, A.E. Qatramez. Energy utilisation in a combined geothermal and organic Rankine power cycles. Int. J. Sustain. Energy 2019, 38, 831–848.
[12] N. Hassani Mokarram, A.H. Mosaffa. Investigation of the thermoeconomic improvement of integrating enhanced geothermal single flash with transcritical organic Rankine cycle. Energy Convers. Manag. 2020, 213, 112831.
[13] G. Liu, Q. Wang, J. Xu, Z. Miao. Exergy Analysis of Two-Stage Organic Rankine Cycle Power Generation System. Entropy 2021, 23, 43. https://doi.org/ 10.3390/e23010043
[14] J.C. Jiménez-García, A. Ruiz, A. Pacheco-Reyes, W.A. Rivera, Comprehensive Review of Organic Rankine Cycles. Processes 2023, 11, 1982. https://doi.org/10.3390/pr11071982
[15] S. Trædal, Analysis of the Trilateral Flash Cycle for Power Production from Low Temperature Heat Sources. Master's Thesis, Institutt for Energi-og Prosessteknikk, Kolbjørn Hejes v 1B, Trondheim, 2014.
[16] C.O.C. Oko and, E.O. Diemuodeke, MS Excel spreadsheet add-in for thermodynamic properties and process simulation of R152a, Energy Science and Technology, Vol. 5, No. 2, 2013, pp. 63-69.
[17] M. Schlueter, J. Rueckmann, M. Gerdts. A Numerical Study of MIDACO on 100 MINLP Benchmarks, Optimization: A Journal of Mathematical Programming and Operations Research, 61,2012,7, 873-900.
[18] MIDACO-Solver, http://www.midaco-solver.com/
[19] M.M. El-Awad, A Solver-TOPSIS technique for multi-objective optimisation of innovative multi-stage VCR systems by using Microsoft Excel, Journal of Engineering Research. Faculty of Engineering-University of Tripoli, Issue (38), November 2024, 25-42, https://www.jer.ly/search_articles.php?f=38
[20] M.J, Moran and H.N. Shapiro, Fundamentals of Engineering Thermodynamics, 5th edition, John Wiley, & Sons. Inc. 2006
[21] M.M. El-Awad, A Multi-Subject Excel Add-In for Fluid Properties and its Use for analysing Cascade and Multi-Stage Compression Refrigeration Cycles, The Electronic Journal of Spreadsheets in Education (eJSiE) Vol. 12, Issue 1, April 18, 2019
[22] ASHRAE Handbook–Refrigeration, 2017, American Society of Heating, Refrigerating and Air-Conditioning Engineers, Inc., (SI Edition).
[23] M.M. El-Awad, M.S. Al Nabhani, K.S. Al Hinai, A. Younis. 2019. Development and Validation of an Excel Add-In for Determining the Properties of Various Refrigerants, Proceedings of First National Conference on Recent Trends in Applied Science, Engineering and Technology (CASET 2K19), Ipri College of Technology, June 11, 2019.